Low-Cost Phased Array Feed System for Radio Astronomy and Wide-Angle Scanning Applications

Sara Salem Hesari
Department of Electrical and Computer Engineering
University of Victoria,
Victoria, BC, Canada
ssalem@uvic.ca

Lisa Locke
Herzberg Astronomy and Astrophysics Research Centre
National Research Council of Canada
Victoria, BC, Canada
llocke@nrao.edu

Lewis Knee
Herzberg Astronomy and Astrophysics Research Centre
National Research Council of Canada
Victoria, BC, Canada
Lewis.Knee@nrc-cnrc.gc.ca

Jens Bornemann
Department of Electrical and Computer Engineering
University of Victoria,
Victoria, BC, Canada
jbornema@ece.uvic.ca

***Abstract*— A low-cost antenna array feed system for 15.4–20.0 GHz is presented. The dual linear polarization, 24-element antenna array and feed network are constructed from single substrate layers, include substrate integrated waveguide-to-microstrip transitions, and coaxial connectors. The individual antennas are arranged on an x-y grid through a metallic backplane that mechanically supports the array and electrically provides a ground plane which reduces back lobes of the end-fire beams and improves directivity. The planar antipodal dipole antenna elements and metal backplane are assembled into a dual linear array, and tested. The phased array's measured results, which are ±40□ scanning range in azimuth and elevation, cross-polar values of 18 dB, wide operating frequency range and flat gain, make the proposed antipodal dipole antenna a viable low-cost candidate for phased array antennas and for use in radio astronomy and wide-angle scanning applications. Measurements are in good agreement with simulations, thus validating the design process.**

Keywords— Phased array, dual polarization, SIW, antipodal, dipole antenna, radio astronomy, scan angle

I. INTRODUCTION

Phased array antennas with wide scan range, high gain, dual polarization capabilities, and end-fire radiation pattern are extensively used in radio astronomy, satellite communications, radar systems, and for military applications. Using substrate integrated waveguide (SIW) for the design of antenna arrays provides the opportunity for low cost, low insertion loss, high quality factor, and ease of component integration on a single substrate layer [1]. Various phased array antennas have been described in the literature, some of which are used for scanning and incorporate phase shifters [2-11]. As an example of some novel wideband antenna designs, a planar 1×8 dipole array has been presented in [2], which served as impetus for our antenna design, having an operating bandwidth of 24–50 GHz. A quasi-rhombus planar antenna with 103% bandwidth which is singly polarized and uses a microstrip line as feed is demonstrated in [3]. A 41-element dual polarized Vivaldi type phased array with integrated low noise CMOS amplifiers is presented in [4] for radio astronomy applications. It is a relatively expensive all-metal antenna design in the lower gigahertz range of 0.7–1.5 GHz.

A number of phased array designs that incorporate wide scanning capabilities and/or an inventive single or dual polarization array have also been studied. One wideband 6–18 GHz, 16-element array of stripline-fed tapered slot antennas integrates couplers and is capable of scanning 60° [5] with a maximum gain of 10 dBi. A dual band slot antenna with a metal cavity on dual-layer substrate achieved a ± 65° scanning range [6]. However, this phased array antenna is only able to scan the E-plane and its fabrication process is complex due to its dual layer structure. A 2×2 and 3×3 series-fed patch array developed for 5G applications at 28 GHz has a gain of 15.2 dBi with ±20° scanning angle [7]. A narrow-band 3-element array scans ±20° by exciting the centre element and changing the reactance of two passive elements [8]. An S-band 1×4 array of patch antennas and loaded line phase shifters is demonstrated in [9], achieving ±30° scanning range with 90° relative phase difference at the antenna inputs. A 4-element phased array with 10 dBi gain in the H-plane is proposed in [10] and steers the beam to -15°, 0°, and 15° by using a reconfigurable defected microstrip structure. A 6×6 dual polarized microstrip phased array is introduced in [11] with 100 MHz bandwidth at 5.2 GHz and ±66° scan range. A wide angle scanning phased array with ±75° is proposed in [12]. This design provides 12.5 dBi gain with 3 dB fluctuations at its operating bandwidth of 5.72–5.87 GHz. A phased array including 312 active elements plus 28 edge elements as feed system for the DRAO 26-metre dish with an operating bandwidth 1–2 GHz is presented.

This paper proposes a phased array antenna system with 24 planar elements arranged in an x-y grid operating from 15.4–20.0 GHz. The SIW antipodal dipole antenna is chosen for the array due to its wide bandwidth, high gain, a reflection coefficient better than 10 dB, low cross-polarization and, most importantly, a wide HPBW of 80° which provides a large scanning range for beam steering applications. A microstrip-to-SIW transition is designed for connecting to coaxial cable. A metallic backplane is used to add mechanical stability and also to reduce back lobe radiation, thus improving the end-fire radiation gain.

The novelty of the proposed 3×3 phased array antenna in comparison with the above-mentioned references is to provide a higher broadside gain of about 21.5 dBi, a ±40° scanning range over a wide bandwidth from 15.4–20 GHz, a symmetrical scan range in both E- and H-planes, and a low-cost and easy fabrication via a printed circuit board process. The proposed dipole antenna array features broad bandwidth,

978-1-7281-3049-1/19/$31.00 ©2019 IEEE

high packing density, no grating lobes [13], low cross polarization of 18 dB as well as low mutual coupling which makes this design suitable for phased array antennas in radio astronomy applications.

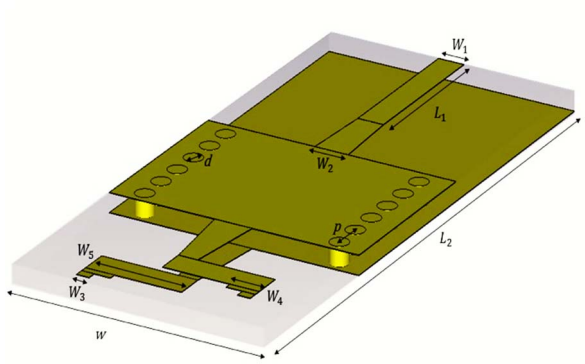

Fig. 1. Planar dipole antenna element with SIW feed layout.

II. Design Procedure

A. Dipole antenna element design

The antipodal dipole antenna was designed on a single substrate layer with SIW feed. The chosen substrate, Rogers RT/Duroid 6002 with relative dielectric constant of 2.94, thickness of 0.508 mm, and loss tangent of 0.0012 at 10 GHz, is mechanically reliable and electrically stable. This dipole antenna was designed using proposed models in [3], [14], and [15]. Fig. 1 shows our design. The SIW width, the thickness of the substrate, the operating frequency, and the dielectric constant are chosen to only excite the TE_{10} mode. Therefore, the electric field, which is vertically polarized in the SIW, starts to gradually rotate between the two arms of the antipodal dipole antenna and provides the horizontal polarization in the aperture of the antenna as shown in Fig. 2.

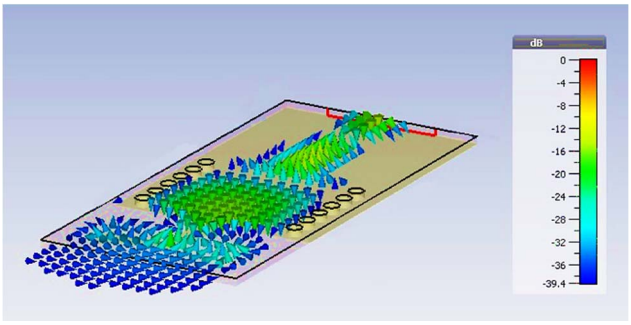

Fig. 2. Planar dipole antenna element's electric field at 17 GHz.

The via diameter d of 0.65 mm is a standard drill size to simplify the low-cost fabrication process. The pitch p (center-to-center spacing between the vias) is 1 mm, resulting in a d/p ratio of 0.65. This ratio must be between 0.5 and 0.8 for minimum leakage and higher efficiency [16]. The equivalent waveguide width of the SIW is calculated according to the formula in [16]; therefore, the centre-to-centre via channel width is 7 mm with its cutoff frequency at 12.49 GHz. A microstrip-to-SIW transition was designed for feeding the dipole antenna as shown in Fig. 1. All antenna and transition dimensions are presented in Table 1.

Fig. 3 presents the reflection coefficient of the antipodal dipole antenna, including all losses, which is better than 10 dB from 15.4–20 GHz with 5.3 dBi gain at the mid-band frequency of 17 GHz. Fig. 4 shows the end-fire radiation pattern of the proposed dipole antenna element at the mid-band frequency. The half power beam width is about 80° over the entire operating bandwidth. The relatively large back lobe will be addressed in the following section.

TABLE.1 Dimensions of the dipole antenna

Parameter	mm	Parameter	mm
W_1	0.92	W	8.98
W_2	1.2	L_1	5.1
W_3	0.4	L_2	19.6
W_4	1	d	0.65
W_5	3.4	p	1

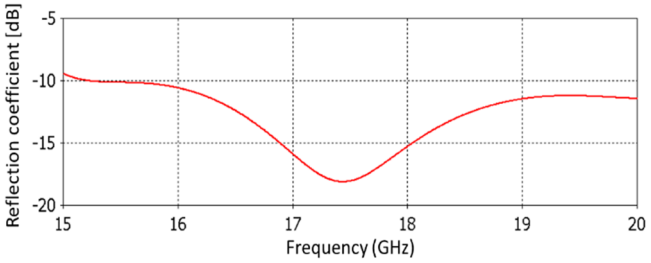

Fig. 3. Simulated reflection coefficient of the planar dipole antenna element.

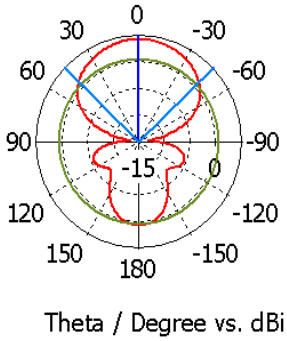

Fig. 4. Fig. 4. Simulated far-field radiation pattern of the planar dipole antenna at 17 GHz.

B. Phased array configuration

Phased array antenna systems used in radio astronomy generally require high gain, low cross polarization, end-fire radiation pattern, polarization purity, low mutual coupling between elements, wide 3 dB beam width, and stable radiation patterns over the entire operating bandwidth [3]. Our antipodal dipole antenna meets these requirements.

A fundamental step in designing a phased array is to define the inter-element spacing d, which is estimated here using the formula for planar arrays [17] and then optimized using CST Microwave Studio. For achieving ±40° beam steering range, a progressive phase shift between adjacent antenna elements is needed. The required phase shift between elements can be calculated as [18]

$$\psi = \frac{-360 f}{c}\left(\left[d_x + \Delta_x\right]\sin\theta\cos\phi + d_y \sin\theta\sin\phi\right) \quad (1)$$

where f is the frequency, c is the speed of light, d_x and d_y are x- and y-element spacings, Δ_x is the row offset for a non-rectangular lattice, and θ and ϕ are the beam steering angles.

The phased array element numbering pattern is shown in Fig. 5a. The antenna elements as assembled into the backplane

978-1-7281-3049-1/19/$31.00 ©2019 IEEE

are shown in Fig. 5b. The backplane adds mechanical stability, ensures element spacing and orthogonality and provides an electrical back plane that reduces the back lobe of the radiation pattern (cf. Fig. 4) and consequently increases the directivity.

The SIW phased array antenna, with a scan angle range of -40° to +40° in both H-plane (azimuth) and E-plane (elevation), was designed and optimized with CST Microwave Studio. All losses including dielectric and copper losses are considered in the simulation results.

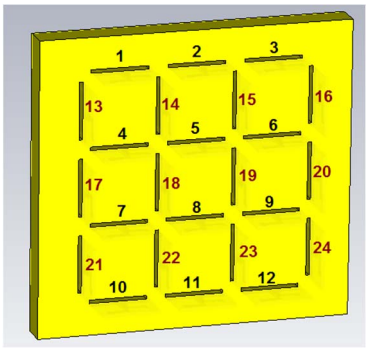

(a)

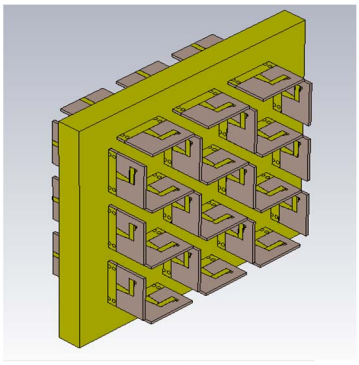

(b)

Fig. 5. 3×3 phased array antenna: (a) element positions including 24 radiating elements, (b) mounted in metallic plate.

Due to the two orthogonal planes of symmetry of the array, only the simulation results of a single quadrant – ports 1, 2, 4, and 5 – are presented. These elements have the same reflection coefficient and active reflection coefficient as other elements due to the array symmetry. Fig. 6 shows the reflection coefficient of the antenna elements 1, 2, 4, and 5. A reflection coefficient better than -10 dB between 16.3–21 GHz was achieved.

The active reflection coefficient is defined as the reflection that a single input port receives while all other elements are excited [5]; in this way the performance of the single antenna in an array environment is predicted. Fig. 7 presents the active reflection coefficients while all horizontal elements numbered 1 to 12 are excited with the same amplitude and phase. The active reflection coefficient of the phased array should be better than 10 dB for all scan angles for the best performance. Therefore, the active reflection coefficient of the system in 30°, 60°, 90°, 120°, 150° and 180° phase differences was simulated.

Fig. 8 depicts the active reflection coefficients of the antenna system when all horizontal antennas are excited with same amplitude and 180° phase difference. The rest of the scan angles give similar performance and are not shown for brevity.

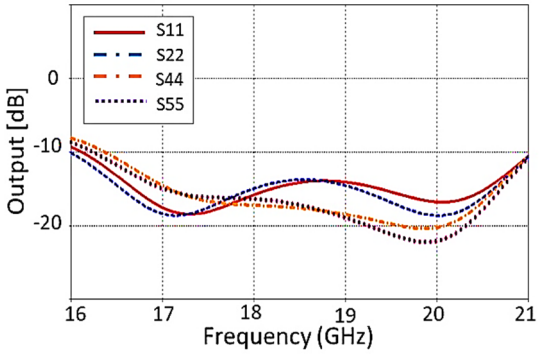

Fig. 6. Reflection coefficients of horizontal elements 1, 2, 4, and 5 of the phased array.

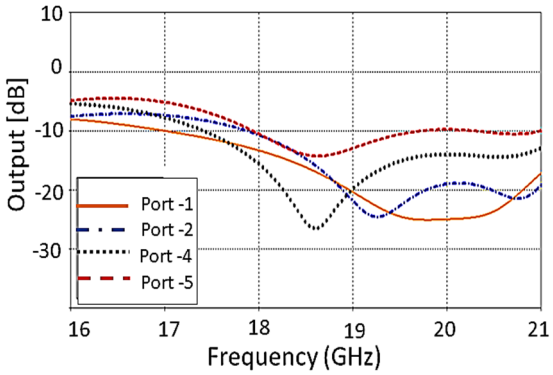

Fig. 7. Active reflection coefficient of one quadrant of horizontal elements 1, 2, 4, and 5, all excited with equal amplitude and phase.

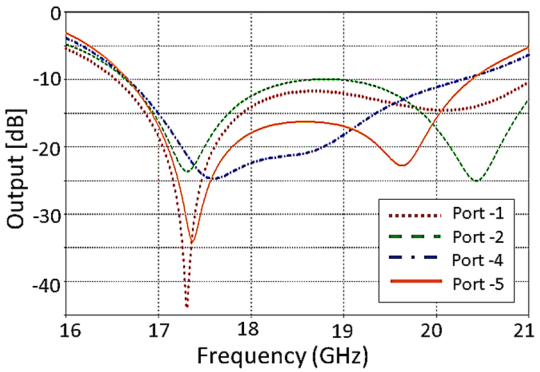

Fig. 8. Active reflection coefficient of one quadrant of horizontal elements 1, 2, 4, and 5 all excited with equal amplitude and 180° phase difference.

High mutual coupling between the elements is the most common problem in designing antenna arrays. Our phased array antenna has low mutual coupling in comparison to some recently proposed phased array antennas such as [5] and [7]. Fig. 9 presents the mutual coupling coefficient of the centre element with respect to all surrounding elements. As is shown in Fig. 9, the mutual coupling coefficient is better than -18 dB between 15–22 GHz and better than -22 dB from 17–21 GHz.

Fig. 10 shows the electric field distribution in all horizontally radiating elements, while vertical ones are terminated by using 50 Ω loads. It is demonstrated that the coupling between horizontal elements 1-12 and vertical elements 13-24 is better than -30 dB.

The system has fairly constant gain over the full bandwidth with a minimum of 19.7 dB (15 GHz) and a maximum of 21.5 dB (20 GHz). It provides 80° scan range,

978-1-7281-3049-1/19/$31.00 ©2019 IEEE

±40° in both vertical and horizontal polarization. Since the array is symmetric, the results are identical for both polarizations. Fig. 11 presents the scan range of the proposed system for six different angles, verifying the beam steering ability of the array.

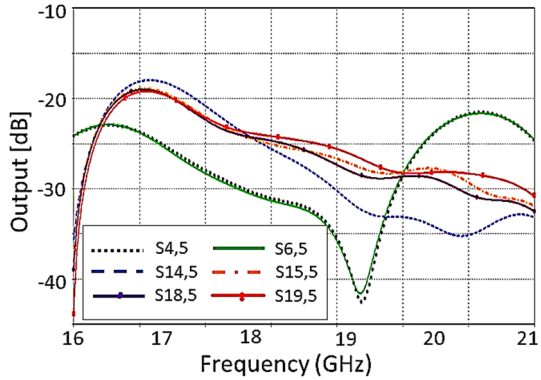

Fig. 9. Mutual coupling coefficient of the centre element 5 with respect to neighbouring elements 4, 6, 14, 15, 18, and 19.

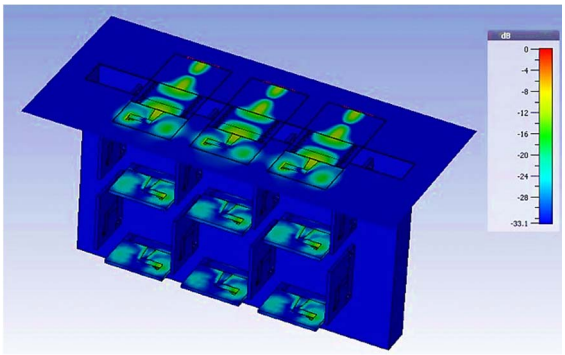

Fig. 10. Electric field of the phased array antenna when all horizontal antennas are excited with same amplitude and phase.

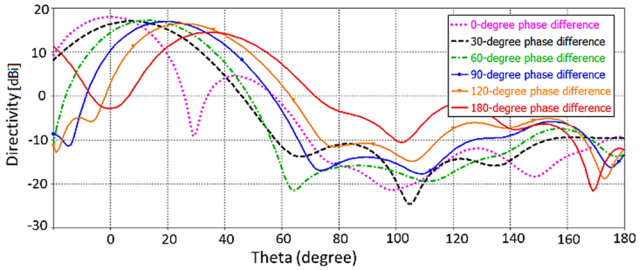

Fig. 11. Scan range of the phased array antenna at 17 GHz (at $\theta = 0$) when applying 0°, 30°, 60°, 90°, 120°, 150°, and 180° phase differences between the neighbouring elements.

III. Experimental Results

The proposed phased array was fabricated and measured in the anechoic chamber of the University of Victoria using an Anritsu 37397C vector network analyzer. Fig. 12 shows the fabricated prototype. Due to lack of equipment and the complexity of exciting all radiating elements at the same time, only the two middle elements were excited in the array structure when verifying the array performance. Two neighbouring elements were chosen to verify the scan range of the system. The center elements usually show the worst mutual coupling in an array since they are surrounded in all directions; thus antenna elements 4 and 5 were chosen for excitation and measurement, and the rest of the ports were terminated with absorber material at the microstrip ports.

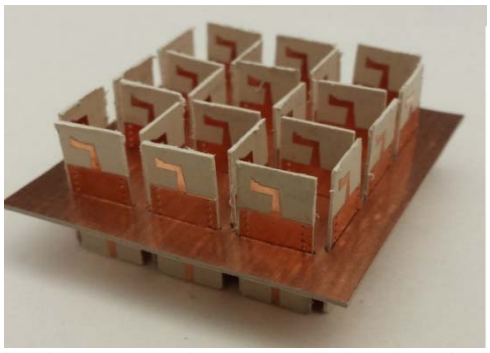

Fig. 12. Phased array antenna elements assembled into back plane.

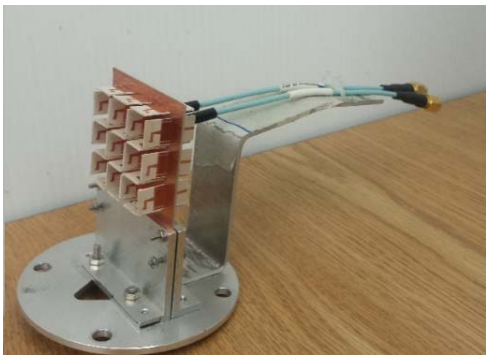

Fig. 13. Phased array antenna and backplane support stand with coaxial cables attached.

For installing the antenna array on the positioner in the anechoic chamber, a support stand was constructed (Fig. 13). Exposed metal sections were covered with absorber material during measurements. A 180° hybrid coupler was used to set the phase differences between elements 4 and 5 to 0° or 180° depending on whether the sum or difference ports were connected, respectively. A broadband quad-ridge Vivaldi horn was used to illuminate the array and provided the ability to measure co-polar and cross-polar radiation patterns.

Fig. 14 shows the simulated and measured radiation patterns of the phased array while exciting ports 4 and 5 with equal amplitude and phase and terminating the unused ports. A directive radiation pattern with 44° HPBW and a maximum measured gain of 11 dBi was obtained. Fig. 15 presents the radiation patterns while exciting ports 4 and 5 with the same amplitude and 180° phase difference. The 180° phase difference causes a deep null at broadside and two main beams with their maxima at -35° and 31°, respectively. The level of the broadside null is measured -30 dB lower than that of the maxima.

As is seen in Fig. 14 and Fig. 15, the measured results are in good agreement with simulations in the main and back lobes. There are some discrepancies in the side lobes which are caused by reflections that are received from the metal positioners on both the transmitter and receiver sides. Due to lack of proper equipment, other phase differences were not measured, but since these results present the minima and maxima of the scan range, it verifies the beam steering ability of this phased array. Since only two antenna elements are excited in this measurement, the scan range is narrower than the earlier claimed value of the full phased array antenna.

978-1-7281-3049-1/19/$31.00 ©2019 IEEE

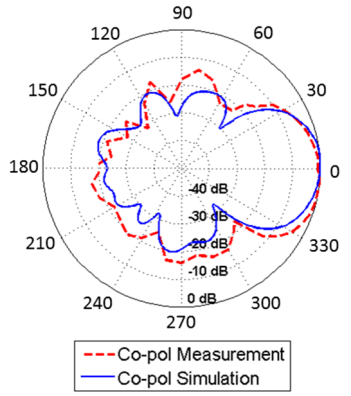

(a)

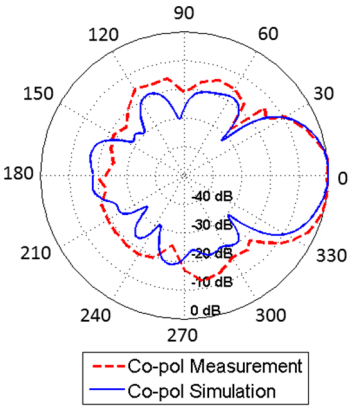

(b)

Fig. 14. Simulated and measured radiation patterns of the phased array antenna while exciting antenna elements 4 and 5 with the same amplitude and 0° phase difference at (a) 18 GHz, (b) 19 GHz.

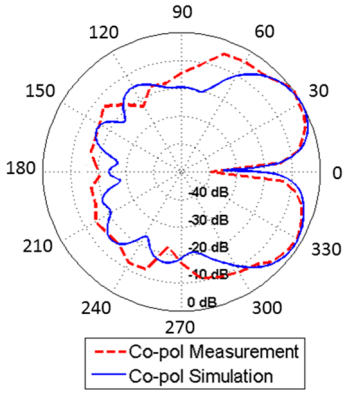

(a)

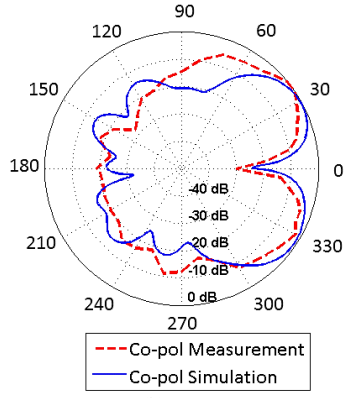

(b)

Fig. 15. Simulated and measured radiation patterns of the phased array antenna while exciting antenna elements 4 and 5 with the same amplitude and 180° phase difference at (a) 18 GHz, (b) 19 GHz.

Fig. 16 presents the measured and simulated co- and cross-polarization levels, showing good agreement, and the cross-polarization value is better than 18 dB in measurements which compares well with the simulations.

Fig. 17 presents the measured and simulated active reflection coefficient of the single antenna element in the phased array with fairly good agreement. The reason for the discrepancy is the fact that the coaxial SMP connectors used for exciting the antenna in the measurement were not included in the simulations.

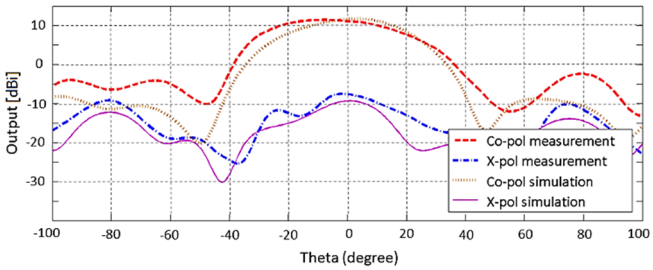

Fig. 16. Co- and cross-polarization of the phased array antenna at 18 GHz.

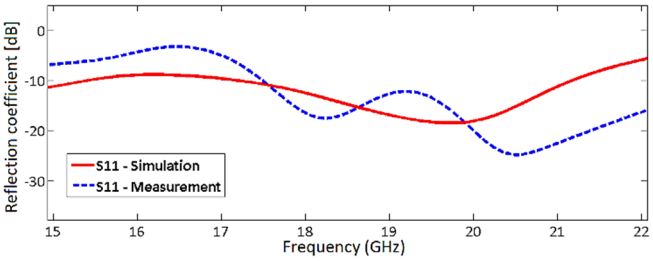

Fig. 17. Active reflection coefficient of the single antenna element in the phased array structure.

IV. Conclusion

We have designed, simulated, and tested a planar antipodal dipole antenna with SIW feed suitable for phased array antenna applications in radio astronomy. It provides a wide bandwidth, good match and wide HPBW over a wide bandwidth. The antipodal dipole is used as a radiating element for a 24-element phased array antenna. A microstrip to SIW transition excites the antenna element, and a coaxial SMP connector is used for feeding the 50-Ω microstrip lines. The array has a ±40° scanning range, cross-polarization of 18 dB, a reflection coefficient better than 10 dB, high gain, and dual polarization without any mechanical rotation. The radiation patterns show the end-fire characteristic of this system with a high directivity of about 18 dB and maximum side lobes of 5 dB at mid-band frequency. The measured results are in good agreement with simulations which confirms the phased array antenna performance and design procedure.

Only a basic SIW feed structure is used in this design. However, it opens the opportunity of having the remaining components such as phase shifters, amplifiers, mixers, etc. on single layers of substrate integrated waveguide. SIW structures make the integration with other planar structures easier and more efficient due to lower loss and more compact structures in comparison to microstrip lines and conventional waveguides, respectively.

V. References

[1] S. Salem Hesari and J. Bornemann, “Wideband circularly polarized substrate integrated waveguide end-fire antenna system with high

gain," IEEE Antennas Wireless Propag. Lett., vol. 16, pp. 2262-2265, 2017.

[2] Y. Wang, H. Wang, and G. Yang, "Design of dipole beam-steering antenna array for 5G handset applications," Proc. Progr. Electromag. Res. Symp., Shanghai, China, Aug. 2016, pp. 2450- 2453.

[3] A. Eldek, "Ultra wideband microstrip antenna for phased array applications," Proc. 37th Eur. Radar Conf., Munich, Germany, Oct. 2007, pp. 319-322.

[4] A. J. Beaulieu, L. Belostotski, T. Burgess, B. Veidt, and J. Haslett, "Noise performance of a phased-array feed with CMOS low-noise amplifiers', IEEE Antennas Wireless Propag. Lett., vol. 15, pp. 1719-1722, 2016.

[5] P. S. Nalumakkal, K. M. Reddy, K. J. Vinoy, and S. Shukla, "Wideband stripline fed tapered slot antenna with integral coupler for wide scan angle active phased array," IET Microw. Antennas Propag., vol. 12, pp. 1487-1493, 2018.

[6] J. Guo, S. Xiao, S. Liao, B. Wang, and D. Xue, "Dual-band and low-profile differentially fed slot antenna for wide-angle scanning phased array," IEEE Antennas Wireless Propag. Lett., vol. 17, pp. 259-262, 2018.

[7] M. Khalily, R. Tafazolli, T. A. Rahman, and M. R. Kamarudin, "Design of phased arrays of series-fed patch antennas with reduced number of the controllers for 28-GHz mm-wave applications," IEEE Antennas Wireless Propag. Lett., vol. 15, pp. 1305-1308, 2016.

[8] Y. Yusuf and X. Gong, 'A low-cost patch antenna phased array with analog beam steering using mutual coupling and reactive loading," IEEE Antennas Wireless Propag. Lett., vol. 7, pp. 81-84, 2008.

[9] M. Nikfalazar, C. Kohler, A. Wiens, A. Mehmood, M. Sohrabi, H. Maune, J. R. Binder, and R. Jacoby, "Beam steering phased array antenna with fully printed phase shifters based on low-temperature sintered BST-composite thick films," IEEE Microw. Wireless Compon. Lett., vol. 26, pp. 70-72, 2016.

[10] C. Ding, Y. J. Guo, P. Y. Qin, and Y.Yang, "A compact microstrip phase shifter employing reconfigurable defected microstrip structure (RDMS) for phased array antennas," IEEE Trans. Antennas Propag., vol. 63, pp. 1985-1996, 2015.

[11] Y. Q. Wen, S. Gao, B. Z. Wang, and Q. Luo, "Dual-polarized and wide-angle scanning microstrip phased array', IEEE Trans. Antennas Propag., vol. 66, pp. 3775-3780, 2018.

[12] C. M. Liu, S. Xiao, and X. L. Zhang, "A compact, low-profile wire antenna applied to wide-angle scanning phased array', IEEE Antennas Wireless Propag. Lett., vol. 17, pp. 389-392, 2018.

[13] B. Veidt and P. Dewdney, "Development of a phased-array feed demonstrator for radio telescopes', Proc. ANTEM Symp., Saint Malo, France, June 2005, pp. 1-4.

[14] H. M. Chen, J. M. Chen, P.S. Cheng, and T. F. Lin, T.F, "Feed for dual-band printed dipole antenna," IET Electron Lett., vol. 40, pp. 1320-1322, 2004.

[15] C. Yu, W. Hong, and Z.Q. Kuai, "Substrate integrated waveguide fed printed dipole array antenna for isolating the RF front-end from the antenna," Microw. Opt. Technol. Lett., vol. 51, pp. 557-562, 2009.

[16] Z. Kordiboroujeni and J. Bornemann, 'Designing the width of substrate integrated waveguide structures," IEEE Microw. Wireless Compon. Lett., vol. 23, pp. 518-520, 2013.

[17] C.A. Balanis, Antenna Theory: Analysis and Design' 3rd ed., John Wiley & Sons, New York, 2005.

[18] Antenna Arrays, Application Note CST STUDIO SUITE™, Sep. 2012.

978-1-7281-3049-1/19/$31.00 ©2019 IEEE